Journal Title
XX(X):1–??
©The Author(s) 2016
Reprints and permission:
sagepub.co.uk/journalsPermissions.nav
DOI: 10.1177/ToBeAssigned
www.sagepub.com/
SAGE

Path reachability including distance-constrained detours

Masahiro Sasabe[1], Miyu Otani[1], Takanori Hara[1], and Shoji Kasahara[1]

Abstract

When nodes and/or links are down in a network, the network may not function normally. Most of the existing work focuses on the reachability between two nodes along a path, i.e., path reliability, and that through arbitrary paths, i.e., network reliability. However, in case of wireless multi-hop networks and road networks, it may be inefficient or difficult to recalculate a path from the source to the destination when a failure occurs at an intermediate link in the path. In such cases, we can expect that the reachability between two nodes will improve by taking detours from the failure point to the destination. Since the detour may also increase the communication/travel delay, in this paper, we propose a new path metric (i.e., path reachability including distance-constrained detours), which consists of the conventional path reachability and the reachability along distance-constrained detours under arbitrary link failures in the original path. We first prove the two important characteristics: 1) the proposed metric is exactly the same as the network reliability in case of no distance constraint and 2) it is upper bounded by the diameter constrained network reliability. Through numerical results using a grid network and more realistic networks (i.e., wireless networks and a road network), we show the fundamental characteristics of the proposed metric and analyze the goodness of several representative paths in terms of the proposed metric as well as the conventional metrics (i.e., path length and path reachability).

Keywords

Path reachability, detour, distance constraint, network reliability, diameter constrained network reliability, wireless network, road network

Introduction

Nowadays, our human society relies on various types of networks such as communication networks and road networks. When some of nodes (e.g., network devices and intersections) and/or links (e.g., communication links and roads) are down, due to failures, natural disasters, or malicious attacks, the network may not be able to work normally. There are many studies on quantitatively evaluating the reliability of the network when the failure probability (or availability) of each node/link is given[1–3]. In this paper, we mainly focus on the link failure.

One possible path reliability metric is the path reliability (reachability), which is defined as the probability that a path $\boldsymbol{r}_{s,t}$ from the source s to the destination t is available (reachable). If the link availability p_e $(0 \leq p_e \leq 1)$ of each link e in $\boldsymbol{r}_{s,t}$ is independent, the path reliability is given by the product of link availability of all links in $\boldsymbol{r}_{s,t}$, i.e., $\prod_{e \in \boldsymbol{r}_{s,t}} p_e$[4]. The s–t network reliability is also a well-known network reliability metric, which is the probability that at least one available path exists from the source s to the destination t[1,2]. In what follows, the s–t network reliability is simply called the network reliability if there is no confusion. The extension of the network reliability with distance (diameter) constraint is called diameter constrained network reliability[5]. The path reliability considers the reachability from s to t under a certain s–t path while the network reliability considers the reachability from s to t under all possible s–t paths.

In case of several situations, e.g., multi-hop communications in wireless networks and evacuation over road networks[4,6,7], when a failure occurs at an intermediate link in the s–t path, taking a detour from the failure point to the destination t will be important/essential to improve the reachability between s and t. Note that taking the detour may increase the total path length, which results in increase of communication delay and travel time, and thus we should consider detour possibility under a certain distance constraint.

In this paper, we introduce a new concept of *distance-constrained detour possibility*, which is the probability that the source s is reachable to the destination t using detours from arbitrary failure points along the given s–t path such that the total path length is equal to or less than a certain threshold. We further formulate a new path metric of *path reachability including distance-constrained detours* as the sum of the conventional path reliability and the distance-constrained detour possibility. We will prove the two important characteristics: 1) the proposed metric is exactly the same as the network reliability in case of no

[1]Nara Institute of Science and Technology, Japan

Corresponding author:
Masahiro Sasabe, Nara Institute of Science and Technology Graduate School of Science and Technology, 8916-5 Takayama-cho, Ikoma, Nara 630-0192, Japan.
Email: m-ssabe@ieee.org

distance constraint and 2) it is upper bounded by the diameter constrained network reliability.

Through numerical experiments using a grid network, we show the fundamental characteristics of the proposed metric and the relation with the existing metrics, i.e., path length, path reliability, and network reliability. We further evaluate the goodness of some representative paths in terms of the proposed metric and existing ones through numerical experiments using realistic networks, i.e., wireless networks and a road network.

The rest of the paper is organized as follows. The following section gives related work, and the subsequent section gives the proposed path metric of the path reachability including distance-constrained detours. A further section demonstrates numerical results using three kinds of networks. The final section provides conclusions and future work.

Related work

Network Reliability Metrics

The s–t network reliability is a representative network reliability metric, which is the probability that at least one available path exists from the source s to the destination t under the assumption where each link in the network independently becomes unavailable at a certain probability[1,2]. The s–t network reliability is also called the 2-terminal network reliability and can be generalized as the k-terminal network reliability, which is the probability that terminals (nodes) in any subset $\mathcal{K}$ of the whole nodes $\mathcal{V}$ in the network ($\mathcal{K} \subseteq \mathcal{V}, k = |\mathcal{K}|$) are reachable with each other[8]. Xiang and Yang[9] proposed the generalized k-terminal network reliability, which is the probability that at least k arbitrary nodes in the network are available and form a connected graph. Petingi and Rodriguez further extended the k-terminal network reliability with the diameter constraint, called the diameter constrained network reliability, which is the probability that the set $\mathcal{K}$ of the whole nodes in the network are reachable through paths of length equal to or less than a certain threshold[5]. Since the computational complexity of the network reliability and its variants are **NP**-hard[10–12], many researchers have studied on efficient algorithms for exact solutions[8,13–15] or those for approximate solutions[16–18].

As for other network reliability metrics, several studies focused on the fraction of important nodes to maintain the network connectivity. Li et al.[19] proposed a new network reliability metric using percolation theory[20,21]. Percolation theory focuses on the network connectivity when part of the nodes and/or links are removed from a network. If a link has capacity (e.g., radio frequency of a wireless link and road width), the link availability depends not only on the failures but also on the capacity. Inoue[3] evaluated the network reliability when using two disjoint s–t paths and proposed a method to detect critical links[22], which have a great impact on the reliability. Detecting critical links will help to analyze how much the network connectivity can be maintained against node/link failures[23].

In this paper, we focus on the path reachability including distance constrained detours, which is the reachability of the s–t path including distance-constrained detours when a link failure occurs at an intermediate link in the s–t path. The concept of the path reachability including distance constrained detours is somewhat similar to that of the diameter constrained network reliability with $k = 2$. The biggest difference is that the former focuses on a certain s–t path and its derived detours while the latter focuses on all the possible paths from s to t. In other words, the diameter constrained network reliability with $k = 2$ will give the upper bound of the path reachability including distance constrained detours. We will also show that the proposed metric without the distance constraint is equivalent to the s–t network reliability. (See details in "Proposed metric" section.)

Path reliability metrics

One possible path reliability metric is the path reliability, which is reachability of an s–t path $\boldsymbol{r}_{s,t}$[4,24]. In wireless sensor networks, communication failures may occur due to environmental noise and/or battery life of sensor nodes[25]. Zonouz et al. proposed the reliability model for each of two types of sensor nodes, i.e., energy-harvesting sensor nodes and battery-powered sensor nodes[26]. They also proposed a link reliability model of the two types of the sensor nodes by considering battery life, shadowing, noise, and positioning errors of global positioning system (GPS). In addition, they analyzed the performance of the shortest distance path, the smallest hop path, and the highest reliable path based on the proposed reliability model, in terms of the number of hops of the path and load balancing. Nowsheen et al.[27] proposed a routing scheme for underwater sensor networks, which considers the number of successfully transmitted packets between sensor nodes, the reachability to a gateway node, and the probability that neighboring sensor nodes exist within the transmission range.

In mobile ad-hoc networks (MANETs), dynamic change of link reliability between nodes due to the node mobility may fail in guaranteeing the quality of service (QoS) of the routing. Chatterjee and Das[28] proposed a dynamic source routing scheme based on the number of hops, congestion degree of a path, and the received signal strength (RSS) of nodes. Kumar and Padmavathy[29] proposed a link reliability model that determines whether a link between two nodes is connected or not based on the Euclidean distance, transmission distance, and the radio propagation characteristics between them. Thanks to this reliability model, they further evaluated the reliability of the shortest path between two nodes.

These existing schemes focus on the reliability of a certain path between two arbitrary nodes but it may be inefficient and/or difficult to reconstruct an alternative s–t path under the occurrence of link failures. In such cases, detours from the failure point to the destination t may improve the s–t reachability. In this paper, we consider the path reachability including distance-constrained detours.

Routing with detours

In wireless sensor networks, each sensor node may not be able to accurately grasp its own location as well as other nodes' locations, which will make data packets encounter a routing hole where there is no node closer to the destination. To address this problem, several studies proposed geographical routing algorithms to transfer data to the destination node by bypassing routing holes[30,31]. Lima et al.[31] proposed a geographic routing algorithm for transferring data to the destination node by bypassing routing holes under the assumption that RSS from the sink node has a positive correlation with the distance to the sink node. Huang et al.[30] proposed an energy-aware geographic routing protocol with bypasses of routing holes for wireless sensor networks with resource constraints.

These schemes can be regarded as reactive ones because they determine a detour after a link failure occurs in the s–t path. On the contrary, in this paper, we focus on a proactive approach, which can evaluate the reachability along the s–t path and its yielding distance-constrained detours in advance.

Proposed metric

Preliminaries

For simplicity of explanation, in what follows, we assume communication networks. Table 1 summarizes the notations used in this paper. $G = (\mathcal{V}, \mathcal{E})$ denotes a directed graph representing the internal structure of a target network, where $\mathcal{V}$ denotes a set of V vertices and $\mathcal{E}$ denotes a set of E directed links. In what follows, we focus on a certain s–t path $\boldsymbol{r}_{s,t}$ in the set $\mathcal{R}_{s,t}$ of all possible s–t paths.

The length $f_{\mathrm{d}}(\boldsymbol{r}_{s,t})$ of the path $\boldsymbol{r}_{s,t}$ is given by the sum of the length of all links in the path $\boldsymbol{r}_{s,t}$:

$$f_{\mathrm{d}}(\boldsymbol{r}_{s,t}) = \sum_{e \in \boldsymbol{r}_{s,t}} d_e,$$

where the path $\boldsymbol{r}_{s,t}$ is given by a vector of links in the path, $(e_1, \ldots, e_{|\boldsymbol{r}_{s,t}|})$, $|\boldsymbol{r}_{s,t}|$ denotes the total number of links in the path $\boldsymbol{r}_{s,t}$, and d_e denotes the length of the link e. Hereinafter, the terms length and distance will be used interchangeably. In case of the communication network, d_e can also be regarded as the propagation delay of the link e. Let $\boldsymbol{d} = (d_1, \ldots, d_E)$ denote a vector of link length.

If the link availability p_e $(0 \leq p_e \leq 1)$ of each link e in an s–t path $\boldsymbol{r}_{s,t}$ is independent, the path reliability (reachability) is defined as follows:

$$f_{\mathrm{p}}(\boldsymbol{r}_{s,t}) = \prod_{e \in \boldsymbol{r}_{s,t}} p_e. \tag{1}$$

Let $\boldsymbol{p} = (p_1, \ldots, p_E)$ denote a vector of link availability.

The s–t network reliability is the probability that at least one available reachable path between s and t exists under the assumption that the link availability of each link $e \in \mathcal{E}$ in the network is independent. The state of the network can be expressed by $\boldsymbol{x} = (x_1, \ldots, x_E) \in \{0,1\}^E$ where $x_e \in \{0,1\}$ represents the state of link e. Each link $e \in \mathcal{E}$ will be available (resp. unavailable), i.e., $x_e = 1$ (resp. $x_e = 0$), with the probability p_e (resp. $(1-p_e)$). The s–t network reliability $f_{\mathrm{N}}(\mathcal{G}_{s,t,G}, \boldsymbol{p})$ can be expressed by the sum of the occurrence probabilities of all events $\mathcal{G}_{s,t,G}$, each of which corresponds to a distinct set of available links such that s is reachable to t. Here, $G_{s,t,G}$ and the occurrence probability $P(\boldsymbol{x})$ are given as follows:

$$\mathcal{G}_{s,t,G} = \big\{\boldsymbol{x} \in \{0,1\}^E \mid \exists \boldsymbol{r}_{s,t} \in \mathcal{R}_{s,t}, \prod_{e \in \boldsymbol{r}_{s,t}} x_e = 1\big\},$$

$$P(\boldsymbol{x}) = \prod_{e \in \mathcal{E}} \left(p_e x_e + (1-p_e)(1-x_e)\right).$$

As a result, $f_{\mathrm{N}}(\mathcal{G}_{s,t,G}, \boldsymbol{p})$ is given by

$$f_{\mathrm{N}}(\mathcal{G}_{s,t,G}, \boldsymbol{p}) = \sum_{\boldsymbol{x} \in \mathcal{G}_{s,t,G}} P(\boldsymbol{x}).$$

Similarly, the diameter constrained network reliability for an s–t pair, $f_{\mathrm{N}}(\mathcal{G}_{s,t,G}(D), \boldsymbol{p})$, can be defined as the sum of the occurrence probabilities of all events $\mathcal{G}_{s,t,G}(D)$ where s is reachable to t along with paths of length equal to or less than a threshold $D \geq 0$. Here, $\mathcal{G}_{s,t,G}(D)$ and $f_{\mathrm{N}}(\mathcal{G}_{s,t,G}(D), \boldsymbol{p})$ are given by

$$\begin{aligned}\mathcal{G}_{s,t,G}(D) = \big\{&\boldsymbol{x} \in \{0,1\}^E \mid \exists \boldsymbol{r}_{s,t} \in \mathcal{R}_{s,t},\\ &\prod_{e \in \boldsymbol{r}_{s,t}} x_e = 1, f_{\mathrm{d}}(\boldsymbol{r}_{s,t}) \leq D\big\},\end{aligned}$$

$$f_{\mathrm{N}}(\mathcal{G}_{s,t,G}(D), \boldsymbol{p}) = \sum_{\boldsymbol{x} \in \mathcal{G}_{s,t,G}(D)} P(\boldsymbol{x}), \tag{2}$$

respectively. Therefore, $f_{\mathrm{N}}(\mathcal{G}_{s,t,G}(\infty), \boldsymbol{p}) = f_{\mathrm{N}}(\mathcal{G}_{s,t,G}, \boldsymbol{p})$.

Detour possibility

Suppose that the lth $(l = 1, \ldots, |\boldsymbol{r}_{s,t}|)$ link $e_l = (u_l, v_l)$ $(u_l, v_l \in \mathcal{V}, u_l \neq v_l)$ in the s–t path $\boldsymbol{r}_{s,t}$ is unavailable. We consider the detour possibility from the node u_l to the destination t along detours that derive from the s–t path $\boldsymbol{r}_{s,t}$ without using the failure link e_l. At first, from (1), we obtain the path reliability of $\boldsymbol{r}^{s,t}_{s,u_l} \subseteq \boldsymbol{r}_{s,t}$ as follows:

$$f_{\mathrm{p}}(\boldsymbol{r}^{s,t}_{s,u_l}) = \prod_{j=1}^{|\boldsymbol{r}^{s,t}_{s,u_l}|} p_{e_j}, \tag{3}$$

where $\boldsymbol{r}^{s,t}_{s,u_l}$ denotes the partial path of $\boldsymbol{r}_{s,t}$ from s to the failure point u_l and we define $\prod_{j=1}^{0} p_{e_j} = 1$. Note that $|\boldsymbol{r}^{s,t}_{s,u_l}| = l-1$. Under the event where the partial path $\boldsymbol{r}^{s,t}_{s,u_l}$ is available and the link e_l is unavailable, the probability that u_l is reachable to t is given by the conditional network reliability $f_{\mathrm{N}}(\mathcal{G}^{\boldsymbol{r}^{s,t}_{s,u_l}, e^0_l}_{u_l,t,G}, \boldsymbol{p})$ under the events $\mathcal{G}^{\boldsymbol{r}^{s,t}_{s,u_l}, e^0_l}_{u_l,t,G}$:

$$\begin{aligned}\mathcal{G}^{\boldsymbol{r}^{s,t}_{s,u_l}, e^0_l}_{u_l,t,G} = \big\{&\boldsymbol{x} \in \{0,1\}^E \mid \boldsymbol{r}^{s,t}_{s,u_l} \in \boldsymbol{r}_{s,t},\\ &\prod_{j=1}^{|\boldsymbol{r}^{s,t}_{s,u_l}|} x_{e_j} = 1, x_{e_l} = 0, \exists \boldsymbol{r}_{u_l,t} \in \mathcal{R}_{u_l,t},\\ &\prod_{e \in \boldsymbol{r}_{u_l,t}} x_e = 1\big\},\end{aligned} \tag{4}$$

$$f_{\mathrm{N}}(\mathcal{G}^{\boldsymbol{r}^{s,t}_{s,u_l}, e^0_l}_{u_l,t,G}, \boldsymbol{p}) = \sum_{\boldsymbol{x} \in \mathcal{G}^{u_l,t}_{\boldsymbol{r}^{s,t}_{s,u_l}, e^0_l}_{s,t,G}} P(\boldsymbol{x}). \tag{5}$$

This event occurs with the probability, which is the product of the path reliability of $\boldsymbol{r}^{s,t}_{s,u_l}$, i.e., (3), and the probability $1 - p_{e_l}$ that link e_l is unavailable. Considering all the

Table 1. Notations.

Notation	Definition
G	Network $G=(\mathcal{V},\mathcal{E})$
$\mathcal{V}$	Set of vertices ($V=\lvert\mathcal{V}\rvert$)
$\mathcal{E}$	Set of links ($E=\lvert\mathcal{E}\rvert$)
d_e	Length of link e
$\boldsymbol{d}$	Vector of link length, $\boldsymbol{d}=(d_1,\ldots,d_E)$
p_e	Availability of link e
$\boldsymbol{p}$	Vector of link availability, $\boldsymbol{p}=(p_1,\ldots,p_E)$
$\boldsymbol{r}_{s,t}$	Certain s–t path, $\boldsymbol{r}_{s,t}=(e_1,\ldots,e_{\lvert\boldsymbol{r}_{s,t}\rvert})$
$\mathcal{R}_{s,t}$	Set of paths from $s\in\mathcal{V}$ to $t\in\mathcal{V}\setminus\{s\}$
$f_{\mathrm{d}}(\boldsymbol{r}_{s,t})$	Length of path $\boldsymbol{r}_{s,t}$
$f_{\mathrm{P}}(\boldsymbol{r}_{s,t})$	Path reliability of $\boldsymbol{r}_{s,t}$
$d_{s,t}^{\min}$	Shortest path length from $s\in\mathcal{V}$ to $t\in\mathcal{V}\setminus\{s\}$
x_e	State of link e: If e is available, $x_e=1$; otherwise, $x_e=0$
$\boldsymbol{x}$	Vector of link state, $\boldsymbol{x}=(x_1,\ldots,x_E)$
$\mathcal{G}_{s,t,G}$	Set of events such that $s\in\mathcal{V}$ and $t\in\mathcal{V}\setminus\{s\}$ are connected
$\mathcal{G}_{s,t,G}(D)$	Set of events such that $s\in\mathcal{V}$ and $t\in\mathcal{V}\setminus\{s\}$ are connected under diameter constraint D
η	Allowable distance increase from the shortest path distance $d_{s,t}^{\min}$
$\boldsymbol{r}_{s,u_l}^{s,t}$	Partial path of $\boldsymbol{r}_{s,t}$ from $s\in\mathcal{V}$ to failure point $u_l\in\mathcal{V}$
$\mathcal{R}_{u_l,t}(d_{s,t}^{\min}+\eta-f_{\mathrm{d}}(\boldsymbol{r}_{s,u_l}^{s,t}))$	Set of distance-constrained detours deriving from failure point $u_l\in\mathcal{V}$
$f_{\mathrm{D}}(\boldsymbol{r}_{s,t})$	Detour possibility of $\boldsymbol{r}_{s,t}$
$f_{\mathrm{D}}(\boldsymbol{r}_{s,t},\eta)$	Detour possibility of $\boldsymbol{r}_{s,t}$ under distance constraint η
$f_{\mathrm{R}}(\boldsymbol{r}_{s,t},\eta)$	Path reachability including distance-constrained detours
$f_{\mathrm{N}}(\mathcal{G}_{s,t,G},\boldsymbol{p})$	s–t network reliability under the set $\boldsymbol{p}$ of link availability
$f_{\mathrm{N}}(\mathcal{G}_{s,t,G}(D),\boldsymbol{p})$	s–t network reliability under the set $\boldsymbol{p}$ of link availability and diameter constraint D

possible events where one of the links, i.e., e_l ($l=1,\ldots,\lvert\boldsymbol{r}_{s,t}\rvert$), in the path $\boldsymbol{r}_{s,t}$ becomes unavailable, we can define the detour possibility $f_{\mathrm{D}}(\boldsymbol{r}_{s,t},\boldsymbol{p})$ of the path $\boldsymbol{r}_{s,t}$ using (3) and (5):

$$f_{\mathrm{D}}(\boldsymbol{r}_{s,t},\boldsymbol{p})=\sum_{l=1}^{\lvert\boldsymbol{r}_{s,t}\rvert} f_{\mathrm{P}}(\boldsymbol{r}_{s,u_l}^{s,t})\cdot(1-p_{e_l})\cdot f_{\mathrm{N}}\big(\mathcal{G}_{u_l,t,G}^{\boldsymbol{r}_{s,u_l}^{s,t},e_l^0},\boldsymbol{p}\big). \tag{6}$$

Path reachability including distance-constrained detours

As for the detour possibility, taking a detour may increase the total length of the s–t path including the detour, which will also increase the communication delay in communication networks (resp. travel time in road networks). In this section, we focus on the distance constrained detour from a failure point to the destination excluding the corresponding failure link.

Suppose that the lth ($l=1,\ldots,\lvert\boldsymbol{r}_{s,t}\rvert$) link $e_l=(u_l,v_l)$ ($u_l,v_l\in\mathcal{V},u_l\neq v_l$) in the path $\boldsymbol{r}_{s,t}$ is unavailable. In case of the detour possibility without the distance constraint, we consider all detour candidates $\mathcal{R}_{u_l,t}$ from the failure point u_l to the destination t excluding e_l. On the other hand, in case of the distance-constrained detour possibility, we need to consider the distance-constrained detour candidates $\mathcal{R}_{u_l,t}(d_{s,t}^{\min}+\eta-f_{\mathrm{d}}(\boldsymbol{r}_{s,u_l}^{s,t}))$ from the failure point u_l to the destination t, which exclude e_l and allow certain distance increase η of the total path length from the shortest path distance $d_{s,t}^{\min}$ between s and t:

$$\mathcal{R}_{u_l,t}(d_{s,t}^{\min}+\eta-f_{\mathrm{d}}(\boldsymbol{r}_{s,u_l}^{s,t}))=\\ \{\boldsymbol{r}_{u_l,t}\mid f_{\mathrm{d}}(\boldsymbol{r}_{s,u_l}^{s,t})+f_{\mathrm{d}}(\boldsymbol{r}_{u_l,t})\leq d_{s,t}^{\min}+\eta,\boldsymbol{r}_{u_l,t}\in\mathcal{R}_{u_l,t}\},$$

where $d_{s,t}^{\min}=\min_{\boldsymbol{r}'_{s,t}\in\mathcal{R}_{s,t}} f_{\mathrm{d}}(\boldsymbol{r}'_{s,t})$ denotes the shortest path distance between s and t and the parameter η denotes the allowable distance increase of the total path from $d_{s,t}^{\min}$. The upper (resp. lower) bound of η is given by $\max_{\boldsymbol{r}'_{s,t}\in\mathcal{R}_{s,t}} f_{\mathrm{d}}(\boldsymbol{r}'_{s,t})-f_{\mathrm{d}}(\boldsymbol{r}_{s,t})$ (resp. $f_{\mathrm{d}}(\boldsymbol{r}_{s,t})-d_{s,t}^{\min}$). The parameter η can control the tradeoff between the total path length and the detour possibility.

Under the event where the path $\boldsymbol{r}_{s,u_l}^{s,t}$ is reachable and the link e_l is unavailable, the probability that u_l is reachable to t under the distance constraint η can be expressed by the conditional network reliability under the events $\mathcal{G}_{u_l,t,G}^{\boldsymbol{r}_{s,u_l}^{s,t},e_l^0}(d_{s,t}^{\min}+\eta-f_{\mathrm{d}}(\boldsymbol{r}_{s,u_l}^{s,t}))$ where $\exists\boldsymbol{r}_{u_l,t}\in\mathcal{R}_{u_l,t}(d_{s,t}^{\min}+\eta-f_{\mathrm{d}}(\boldsymbol{r}_{s,u_l}^{s,t}))$ is connected. Here, $\mathcal{G}_{u_l,t,G}^{\boldsymbol{r}_{s,u_l}^{s,t},e_l^0}(d_{s,t}^{\min}+\eta-f_{\mathrm{d}}(\boldsymbol{r}_{s,u_l}^{s,t}))$ and $f_{\mathrm{N}}(\mathcal{G}_{u_l,t,G}^{\boldsymbol{r}_{s,u_l}^{s,t},e_l^0}(d_{s,t}^{\min}+\eta-f_{\mathrm{d}}(\boldsymbol{r}_{s,u_l}^{s,t})),\boldsymbol{p})$ are given as follows:

$$\mathcal{G}_{u_l,t,G}^{\boldsymbol{r}_{s,u_l}^{s,t},e_l^0}(d_{s,t}^{\min}+\eta-f_{\mathrm{d}}(\boldsymbol{r}_{s,u_l}^{s,t}))=\\ \{\boldsymbol{x}\in\{0,1\}^E\mid \boldsymbol{r}_{s,u_l}^{s,t}\in\boldsymbol{r}_{s,t},\\ \prod_{j=1}^{\lvert\boldsymbol{r}_{s,u_l}^{s,t}\rvert} x_{e_j}=1, x_{e_l}=0,\exists\boldsymbol{r}_{u_l,t}\in\mathcal{R}_{u_l,t},\\ \prod_{e\in\boldsymbol{r}_{u_l,t}} x_e=1, f_{\mathrm{d}}(\boldsymbol{r}_{s,u_l}^{s,t})+f_{\mathrm{d}}(\boldsymbol{r}_{u_l,t})\leq d_{s,t}^{\min}+\eta\},$$

$$f_{\mathrm{N}}(\mathcal{G}_{u_l,t,G}^{\boldsymbol{r}_{s,u_l}^{s,t},e_l^0}(d_{s,t}^{\min}+\eta-f_{\mathrm{d}}(\boldsymbol{r}_{s,u_l}^{s,t})),\boldsymbol{p}) = \sum_{\boldsymbol{x}\in\mathcal{G}_{u_l,t,G}^{\boldsymbol{r}_{s,u_l}^{s,t},e_l^0}(d_{s,t}^{\min}+\eta-f_{\mathrm{d}}(\boldsymbol{r}_{s,u_l}^{s,t}))} P(\boldsymbol{x}). \quad (7)$$

From (3) and (7), we can define the detour possibility under the distance constraint η as follows:

$$f_{\mathrm{D}}(\boldsymbol{r}_{s,t},\boldsymbol{p},d_{s,t}^{\min}+\eta) = \sum_{l=1}^{|\boldsymbol{r}_{s,t}|} f_{\mathrm{p}}(\boldsymbol{r}_{s,u_l}^{s,t})\cdot(1-p_{e_l})\cdot f_{\mathrm{N}}(\mathcal{G}_{u_l,t,G}^{\boldsymbol{r}_{s,u_l}^{s,t},e_l^0}(d_{s,t}^{\min}+\eta-f_{\mathrm{d}}(\boldsymbol{r}_{s,u_l}^{s,t})),\boldsymbol{p}). \quad (8)$$

The path reachability including the distance-constrained detours of $\boldsymbol{r}_{s,t}$, $f_{\mathrm{R}}(\boldsymbol{r}_{s,t},\boldsymbol{p},\eta)$, can be expressed by the sum of (1) and (8):

$$f_{\mathrm{R}}(\boldsymbol{r}_{s,t},\boldsymbol{p},d_{s,t}^{\min}+\eta) = f_{\mathrm{p}}(\boldsymbol{r}_{s,t}) + f_{\mathrm{D}}(\boldsymbol{r}_{s,t},\boldsymbol{p},d_{s,t}^{\min}+\eta). \quad (9)$$

Here, we provide the following important theorems related to the path reachability including the distance-unconstrained detours.

Theorem 1. *Given a certain path $\boldsymbol{r}_{s,t}$, the path reachability including the distance-unconstrained detours of $\boldsymbol{r}_{s,t}$, $f_{\mathrm{R}}(\boldsymbol{r}_{s,t},\boldsymbol{p},\infty)$, is exactly same as the s–t network reliability $f_{\mathrm{N}}(\mathcal{G}_{s,t,G},\boldsymbol{p})$:*

$$f_{\mathrm{R}}(\boldsymbol{r}_{s,t},\boldsymbol{p},\infty) = f_{\mathrm{N}}(\mathcal{G}_{s,t,G},\boldsymbol{p}).$$

The proof will be given in "Proof to Theorem 1" section.

Theorem 2. *Given a certain path $\boldsymbol{r}_{s,t}$ and $\eta \geq \eta_0$ such that $f_{\mathrm{d}}(\boldsymbol{r}_{s,t}) = d_{s,t}^{\min}+\eta_0$, the s–t diameter constrained network reliability $f_{\mathrm{N}}(\mathcal{G}_{s,t,G}(d_{s,t}^{\min}+\eta),\boldsymbol{p})$ gives the upper bound of the path reachability including the distance-constrained detours of $\boldsymbol{r}_{s,t}$, $f_{\mathrm{R}}(\boldsymbol{r}_{s,t},\boldsymbol{p},d_{s,t}^{\min}+\eta)$:*

$$f_{\mathrm{R}}(\boldsymbol{r}_{s,t},\boldsymbol{p},d_{s,t}^{\min}+\eta) \leq f_{\mathrm{N}}(\mathcal{G}_{s,t,G}(d_{s,t}^{\min}+\eta),\boldsymbol{p}).$$

The proof will be given in "Proof to Theorem 2" section.

Numerical experiments

In this section, we first show the fundamental characteristics of the the proposed metric (i.e., path reachability including distance-constrained detours) through evaluations under a grid network. Then, we further evaluate the goodness of some representative paths in terms of the path length, path reliability, and proposed metric, under wireless networks and a road network.

Evaluation model

Since the computation of the network reliability is **NP**-hard, multiple algorithms have been proposed to tackle the computational complexity[32,33]. In this paper, we use Graphillion[34], which is a Python library for efficiently computing the network reliability utilizing a zero-suppressed binary decision diagram (ZDD)[35]. ZDD is one of the compressed data structures for a family of sets. As for the evaluation networks, we use three kinds of networks, i.e., a grid network, wireless networks, and a road network.

Fundamental characteristics of proposed metric

We first reveal the fundamental characteristics of the path reachability including distance-constrained detours through numerical experiments using a grid network. Fig. 1 illustrates the 5×5 grid network for evaluation, where the length of each link is set to be 1. We set the availability of each link e highlighted in red color (i.e., located at the central 3×5 region) to be $p_e=0.9$ and that of each remaining link e to be $p_e=0.99$. As a result, all s–t paths will be required to traverse the low-availability area. We select two representative s–t paths, $\boldsymbol{r}_{s,t}^1$ (a blue line) and $\boldsymbol{r}_{s,t}^2$ (a green line), both of which are the shortest path and have the same path reliability.

Fig. 2 depicts the transition of the path reachability including distance-constrained detours of $\boldsymbol{r}_{s,t}^1$ and that of $\boldsymbol{r}_{s,t}^2$ when changing the allowable distance increase η from the shortest path distance $d_{s,t}^{\min}$. For comparison purpose, we also show the path reliability of $\boldsymbol{r}_{s,t}^1$ and $\boldsymbol{r}_{s,t}^2$, network reliability, and diameter constrained network reliability. Recall that the path reliability and the path reachability including distance-constrained detours are path reliability metrics, which depend on the s–t path, i.e., $\boldsymbol{r}_{s,t}^1$ and $\boldsymbol{r}_{s,t}^2$, while the network reliability and the diameter constrained network reliability are the network reliability metrics, which depend on the s–t pair. We first observe that the path reachability including distance-constrained detours monotonically increases with η. From (9), recall that the difference from the path reachability including distance-constrained detours with η to the path reliability is exactly same as the distance-constrained detour possibility with η. For example, when $\eta=0$, we observe from the figure that the distance-constrained detour possibility of $\boldsymbol{r}_{s,t}^1$ (resp. $\boldsymbol{r}_{s,t}^2$) is represented by the blue vertical arrow (resp. green vertical arrow) and becomes 0.196 (resp. 0.038). Since $\boldsymbol{r}_{s,t}^1$ always shows higher path reachability including distance constrained detours than $\boldsymbol{r}_{s,t}^2$, it can be regarded as a better path in terms of distance-constrained detours. This is because $\boldsymbol{r}_{s,t}^1$ adopts the links located at the center of the network and can have abundant detour candidates, compared with $\boldsymbol{r}_{s,t}^2$. This simple example demonstrates that the proposed metric matches well with the intuitive understanding and can quantitatively evaluate the goodness of a certain path in terms of the distance-constrained detours.

We also confirm that the path reachability including distance-constrained detours of $\boldsymbol{r}_{s,t}^1$ and $\boldsymbol{r}_{s,t}^2$ is always upper bounded by the diameter constrained network reliability and approaches the s–t network reliability with increase of η. These phenomena can be regarded as the numerical verification of the proof in Appendices and .

Numerical examples of proposed metric for representative paths under realistic networks

In this section, we evaluate the goodness of some representative paths under realistic networks, i.e., wireless networks and a road network, in terms of the path length, path reliability, and path reachability including distance-constrained detours. It is difficult to evaluate the distance-constrained detour possibility of all possible s–t paths due to the computational complexity. In addition, taking detours will be required only when some failure occurs on the

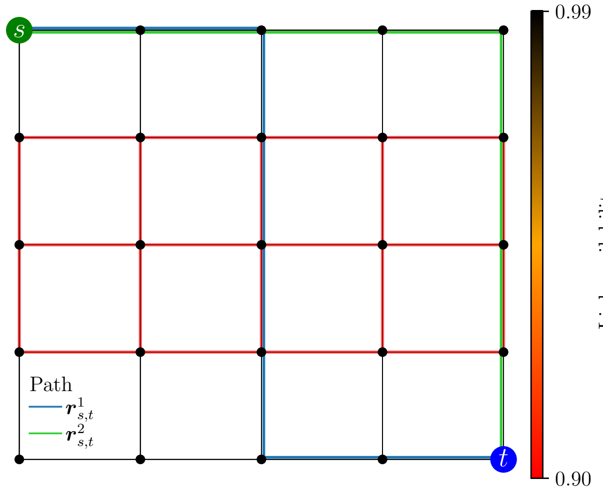

Figure 1. Grid network ($V = 25$, $E = 40$).

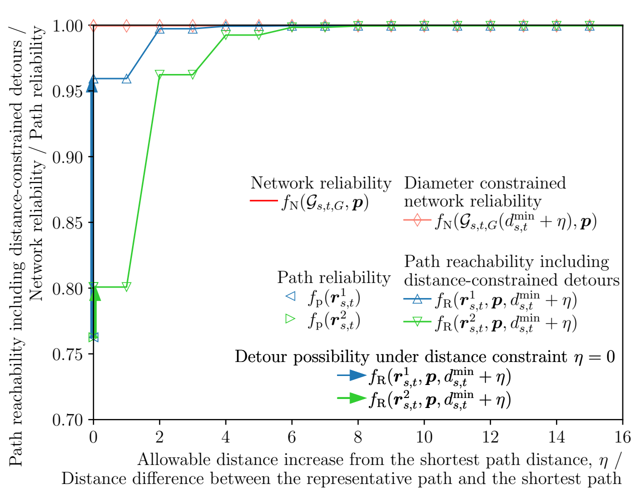

Figure 2. Impact of η on path reachability including distance-constrained detours of $\boldsymbol{r}^1_{s,t}$ and $\boldsymbol{r}^2_{s,t}$ (grid network case).

original path. In other words, the original path should have good properties in terms of the existing path metrics, i.e., path length and path reliability. Considering these points, we focus on the five representative paths, i.e., the shortest path $\boldsymbol{r}^{d_{\min}}_{s,t}$, the path with the highest path reliability, $\boldsymbol{r}^{p_{\max}}_{s,t}$, and three paths taking account of the balance between path reliability and path length: $\boldsymbol{r}^{\mathrm{B1}}_{s,t}$, $\boldsymbol{r}^{\mathrm{B2}}_{s,t}$, and $\boldsymbol{r}^{\mathrm{B3}}_{s,t}$. $\boldsymbol{r}^{\mathrm{B1}}_{s,t}$, $\boldsymbol{r}^{\mathrm{B2}}_{s,t}$, and $\boldsymbol{r}^{\mathrm{B3}}_{s,t}$ are calculated as follows. We first enumerate all possible s–t paths $\boldsymbol{r}_{s,t} \in \mathcal{R}_{s,t}$ except $\boldsymbol{r}^{d_{\min}}_{s,t}$ and $\boldsymbol{r}^{p_{\max}}_{s,t}$ in descending order of the path reliability. Then, we select three paths out of the sorted path candidates such that the selected path $\boldsymbol{r}_{s,t}$ should satisfy the distance condition $f_{\mathrm{d}}(\boldsymbol{r}_{s,t}) \le f_{\mathrm{d}}(\boldsymbol{r}^{p_{\max}}_{s,t})$. Note that the selected paths are labeled as $\boldsymbol{r}^{\mathrm{B1}}_{s,t}$, $\boldsymbol{r}^{\mathrm{B2}}_{s,t}$, and $\boldsymbol{r}^{\mathrm{B3}}_{s,t}$ in ascending order of their path length.

Evaluation under wireless networks As for wireless networks, we use a unit disk graph model[36], which has widely been used for modeling MANETs and sensor networks[37,38]. In the unit disk graph, nodes with transmission range R ($R > 0$) are randomly distributed in the two-dimensional Euclidean space and two nodes are considered to be connected (i.e., have a link) if their Euclidean distance is equal to or less than R, i.e., they are located within the transmission range with each other. We generate 25 unit disk graphs with 35 nodes ($V = 35$), identical transmission range ($R = 0.25$), and area size of 1×1. Note that the number E of links will be determined by the geographical locations of nodes. Fig. 3 illustrates one example among 25 networks, i.e., wireless network 1, where $V = 35$ and $E = 70$.

We randomly select 60% links as "less reliable" and the remaining as "more reliable." In particular, each less (resp. more) reliable link e has link availability p_e following a uniform distribution in the range of $[0.80, 0.95]$ (resp. $[0.998, 1.0]$) as in the existing work[39]. We set the source node s (resp. destination node t) to the node closest to the upper left (resp. lower right) of the network. We also show the five representative paths in Fig. 3. Since they share some links with others, their locations are adjusted to avoid the overlapping as much as possible.

Fig. 4 illustrates the impact of η on the path reachability including distance-constrained detours of the five representative paths in wireless network 1. For comparison purpose, we also show the network reliability, diameter constrained network reliability, and path reliability of them. Note that unlike with Fig. 2, the path reliability becomes different among the five paths. As for each path except the shortest path, i.e., $\boldsymbol{r}^{p}_{s,t}$ ($p \in \{p_{\max}, \mathrm{B1}, \mathrm{B2}, \mathrm{B3}\}$), we show a vertical arrow from the point of the path reachability $f_{\mathrm{P}}(\boldsymbol{r}^{p}_{s,t})$ to that of the path reachability including distance-constrained detours with $\eta = \eta^{p}_{0}$, i.e., $f_{\mathrm{R}}(\boldsymbol{r}^{p}_{s,t}, \boldsymbol{p}, d^{\min}_{s,t} + \eta^{p}_{0})$, where η^{p}_{0} is the difference of path length between $\boldsymbol{r}^{p}_{s,t}$ and $\boldsymbol{r}^{d_{\min}}_{s,t}$, i.e., $f_{\mathrm{d}}(\boldsymbol{r}^{p}_{s,t}) - f_{\mathrm{d}}(\boldsymbol{r}^{d_{\min}}_{s,t})$. Note that we omit the vertical arrow for $\boldsymbol{r}^{d_{\min}}_{s,t}$ because its arrow length becomes zero. The length of the vertical arrow for $\boldsymbol{r}^{p}_{s,t}$ presents the lower bound of the distance-constrained detour possibility, $f_{\mathrm{D}}(\boldsymbol{r}_{s,t}, d^{\min}_{s,t} + \eta^{p}_{0})$, (i.e., the difference between the lower bound of the path reachability including distance-constrained detours $f_{\mathrm{R}}(\boldsymbol{r}^{p}_{s,t}, \boldsymbol{p}, d^{\min}_{s,t} + \eta^{p}_{0})$ and path reliability $f_{\mathrm{P}}(\boldsymbol{r}^{p}_{s,t})$) for the corresponding path $\boldsymbol{r}^{p}_{s,t}$. Note that unlike with Fig. 2, each path $\boldsymbol{r}^{p}_{s,t}$ has the different path length, and thus the corresponding η_p also differs. The long (resp. small) vertical arrow indicates that the corresponding path can drastically (resp. slightly) improve the reachability thanks to the detours without increasing the total path length. In this aspect, we confirm that the representative paths except the shortest path are attractive.

We also observe that the path reachability including distance-constrained detours monotonically increases with η, regardless of the paths. In particular, we confirm that the path reachability including distance-constrained detours of $\boldsymbol{r}^{\mathrm{B1}}_{s,t}$ can be improved by 6.53%, compared with that of $\boldsymbol{r}^{p_{\max}}_{s,t}$, when $\eta = 0.35$. Since $\boldsymbol{r}^{\mathrm{B1}}_{s,t}$ also has shorter path length than $\boldsymbol{r}^{p_{\max}}_{s,t}$ at the slight decrease of the path reachability, it can be viewed as an attractive path. We also confirm that the diameter constrained network reliability gives the upper bound of the path reachability including distance-constrained detours, regardless of the paths.

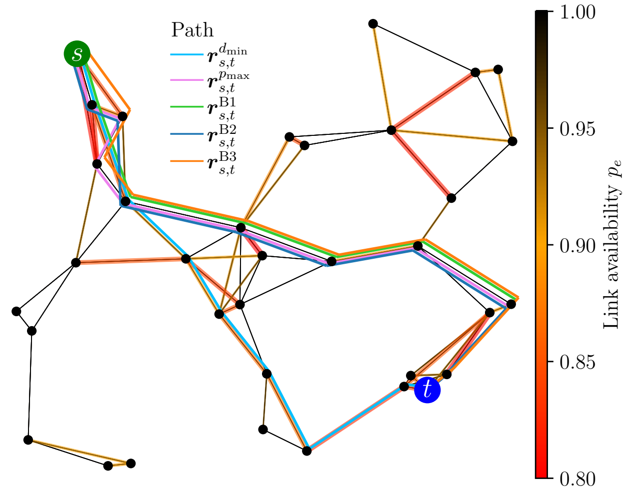

Figure 3. Wireless network 1 ($V = 35$, $E = 70$).

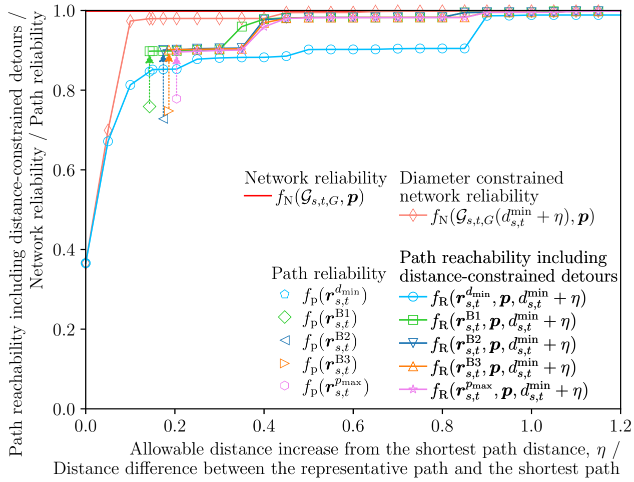

Figure 4. Impact of η on path reachability including distance-constrained detours (Wireless network 1).

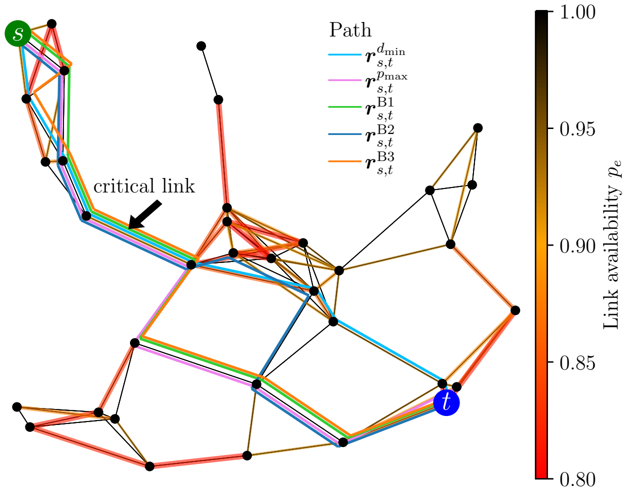

Figure 5. Wireless network 2 ($V = 35$, $E = 86$).

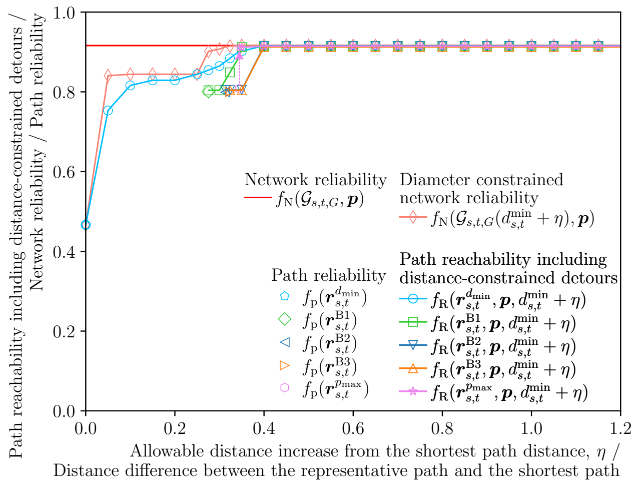

Figure 6. Impact of η on path reachability including distance-constrained detours (Wireless network 2).

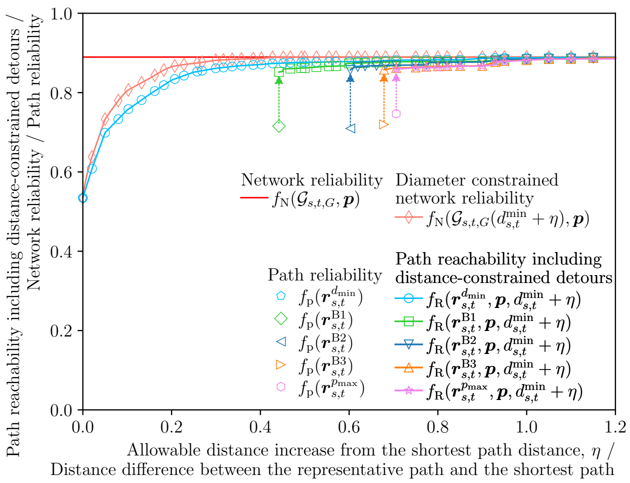

Figure 7. Impact of η on path reachability including distance-constrained detours (Average of 25 wireless networks).

Next, we focus on another network example (wireless network 2) with five representative paths, as shown in Fig. 5. Fig 6 illustrates the impact of η on the path reachability including distance-constrained detours of the five representative paths in wireless network 2. As in Fig 4, we also give the network reliability, diameter constrained network reliability, and path reliability of them. As for the vertical arrow, we only show it for $\boldsymbol{r}_{s,t}^{p_{\max}}$. We observe that the lower bound $f_{\mathrm{D}}(\boldsymbol{r}_{s,t} d_{s,t}^{\min} + \eta_0^p)$ of the path reachability including distance-constrained detours of path $\boldsymbol{r}_{s,t}^p$ ($p \in \{d_{\min}, \mathrm{B1}, \mathrm{B2}, \mathrm{B3}\}$) exhibits almost the same performance as the path reliability $f_{\mathrm{P}}(\boldsymbol{r}_{s,t}^p)$ of $\boldsymbol{r}_{s,t}^p$. This phenomenon stems from the structure of wireless network 2 where every s–t path must pass through a crucial link, which is designated in Fig. 6, and thus taking detours becomes difficult.

As for the impact of η on the path reachability including distance-constrained detours, we confirm the similar tendency observed in Fig. 4. In this case, $\boldsymbol{r}_{s,t}^{p_{\max}}$ shows relatively good characteristics from the viewpoint of both the path reliability and path reachability including distance-constrained detours.

So far we have focused on wireless networks 1 and 2 as illustrative examples. Finally, we demonstrate more

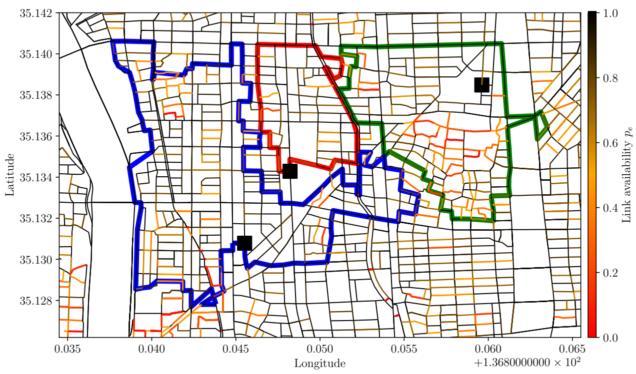

Figure 8. Road network ($2,640\,[\mathrm{m}] \times 1,690\,[\mathrm{m}]$ area of Nagoya city in Japan) with three refuge areas: Area 1 ($1,220\,[\mathrm{m}] \times 960\,[\mathrm{m}]$ green area), Area 2 ($540\,[\mathrm{m}] \times 740\,[\mathrm{m}]$ red area), Area 3 ($1,680\,[\mathrm{m}] \times 1,500\,[\mathrm{m}]$ blue area).

general results by showing the average results of 25 wireless networks, as shown in Fig. 7. We confirm that the trends observed in the two examples hold.

Evaluation under a road network We consider an evacuation situation under a large-scale disaster. In Japan, a municipality, e.g., Nagoya city, has been assessing the potential blockage risk of each road in its administrative area under large-scale disasters, e.g., earthquake. More specifically, using a mathematical model, it gives the road blockage probability p'_e $(0 \le p'_e \le 1)$ that the road $e \in \mathcal{E}$ is blocked by collapsed roadside buildings due to an earthquake[40]. In this case, we can regard the availability p_e of each link $e \in \mathcal{E}$ as $1 - p'_e$.

Fig. 8 shows the road network of $2,640\,[\mathrm{m}] \times 1,690\,[\mathrm{m}]$ Arako area of Nagoya city in Japan[40]. This area is further divided into three refuge areas using the existing refuge assignment scheme[41]: Area 1 ($1,220\,[\mathrm{m}] \times 960\,[\mathrm{m}]$ green area), Area 2 ($540\,[\mathrm{m}] \times 740\,[\mathrm{m}]$ red area), and Area 3 ($1,680\,[\mathrm{m}] \times 1,500\,[\mathrm{m}]$ blue area). We also show the availability p_e of each link e.

In each area $a \in \{1,2,3\}$, we prepare three evacuation situations where an evacuee moves from a certain position $s = s_{a,i}$ $(i \in \{1,2,3\})$ (a green point) to the corresponding refuge $t = t_a$ (a blue point), as shown in Figs. 9a–11a for Area 1, Figs. 12a–14a for Area 2, and Figs. 15a–17a for Area 3. Note that Figs. 10 through 17 are given as the supplemental materials. In each figure, we also show the five representative paths: the shortest path $\boldsymbol{r}^{d_{\min}}_{s,t}$, the path with the highest path reachability, $\boldsymbol{r}^{p_{\max}}_{s,t}$, and three paths taking account of the balance between path reliability and path length: $\boldsymbol{r}^{\mathrm{B1}}_{s,t}$, $\boldsymbol{r}^{\mathrm{B2}}_{s,t}$, and $\boldsymbol{r}^{\mathrm{B3}}_{s,t}$. Considering the computational complexity to calculate the path reachability including distance-constrained detours using ZDD, we first extract the part of the road network in a minimum polygon shape such that the extracted road network includes the five representative paths.

Fig. 9b illustrates the impact of η on the path reachability including distance-constrained detours of the five representative paths in case of Area 1 with $s = s_{1,1}$ and $t = t_1$. As in Fig 4, we also give the network reliability, diameter constrained network reliability, and path reliability of them. As for the vertical arrows, we show them for $\boldsymbol{r}^{p}_{s,t}$ $(p \in \{p_{\max}, \mathrm{B1}, \mathrm{B2}, \mathrm{B3}\})$. We first observe that $\boldsymbol{r}^{p}_{s,t}$ $(p \in \{p_{\max}, \mathrm{B1}, \mathrm{B2}, \mathrm{B3}\})$ has 25.35–27.13 (resp. 1.19–1.19) times as large path reliability (resp. long path length) as $\boldsymbol{r}^{d_{\min}}_{s,t}$. From the viewpoint of the path reachability including distance-constrained detours, $\boldsymbol{r}^{p}_{s,t}$ $(p \in \{d_{\min}, \mathrm{B1}, \mathrm{B2}\})$ always outperforms $\boldsymbol{r}^{p'}_{s,t}$ $(p' \in \{p_{\max}, \mathrm{B3}\})$. As a result, in this case, we think $\boldsymbol{r}^{\mathrm{B1}}_{s,t}$ and $\boldsymbol{r}^{\mathrm{B2}}_{s,t}$ are well-balanced in terms of the path length, path reliability, and distance-constrained detour possibility.

We can confirm the similar tendency in other cases as shown in Figs. 10 through 17 in the supplemental materials.

Conclusion

In this paper, we have proposed a new concept of *distance-constrained detour possibility*, which is the probability that the source s is reachable to the destination t using detours such that the total path length including a detour is equal to or less than a certain threshold. We have further formulated a new path metric of *path reachability including distance-constrained detours* as the sum of the path reliability and the distance-constrained detour possibility. We have proved that 1) the proposed metric is equivalent to the network reliability in case of no distance constraint and 2) it is upper bounded by the diameter constrained network reliability.

Through numerical experiments using a grid network, we have shown the fundamental characteristics of the path reachability including distance-constrained detours and the relation with the network reliability and diameter constrained network reliability. We have further evaluated the goodness of five representative paths, i.e., the shortest path, the most reliable path, and three paths taking account of the balance between path reliability and path length, through numerical experiments using realistic networks, i.e., wireless networks and a road network. We have shown that some of the representative paths can be well-balanced paths for these networks in terms of the path length, path reliability, and path reachability including distance-constrained detours.

In future work, we plan to tackle the computation complexity problem of calculating path reachability including distance-constrained detours, with the help of approximation methods for network reliability, e.g., Monte Carlo based approaches.

Proof to Theorem 1

Proof. For simplicity of explanation, we define H as the total number of links in the path $\boldsymbol{r}_{s,t}$, i.e., $H = |\boldsymbol{r}_{s,t}|$. Considering all the possible events where one of the links, $e_l = (u_l, v_l)$ $(l = 1, \ldots, H, u_l, v_l \in \mathcal{V}, u_l \ne v_l)$, in the path $\boldsymbol{r}_{s,t}$ becomes unavailable, we can express the detour possibility of the path $\boldsymbol{r}_{s,t}$ using (6):

$$f_{\mathrm{D}}(\boldsymbol{r}_{s,t}, \boldsymbol{p}) = \sum_{l=1}^{H} f_{\mathrm{P}}\left(\boldsymbol{r}^{s,t}_{s,u_l}\right) \cdot (1 - p_{e_l}) \cdot f_{\mathrm{N}}\left(\mathcal{G}^{\boldsymbol{r}^{s,t}_{s,u_l}}_{u_l,t,G}, \boldsymbol{p}\right) \quad (10)$$

From (9), we obtain the path reachability including distance-constrained detours with $\eta = \infty$ as follows:

$$\begin{aligned} f_{\mathrm{R}}(\boldsymbol{r}_{s,t}, \boldsymbol{p}, \infty) &= f_{\mathrm{P}}(\boldsymbol{r}_{s,t}) + f_{\mathrm{D}}(\boldsymbol{r}_{s,t}, \boldsymbol{p}, \infty) \\ &= f_{\mathrm{P}}(\boldsymbol{r}_{s,t}) + f_{\mathrm{D}}(\boldsymbol{r}_{s,t}, \boldsymbol{p}). \end{aligned}$$

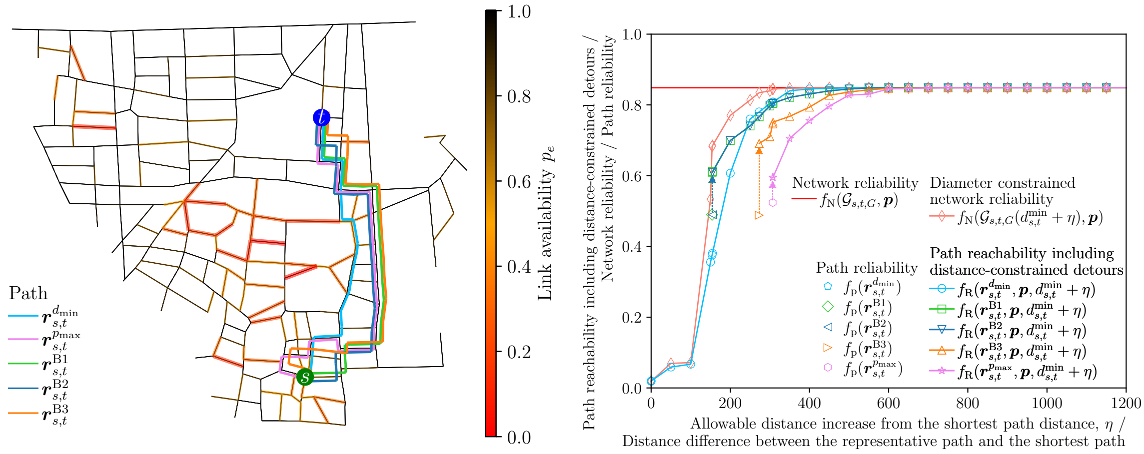

(a) Network topology and five representative paths.

(b) Impact of η on path reachability including distance-constrained detours.

Figure 9. Results of road network (Area 1, $s = s_{1,1}, t = t_1$).

Here, we define the following two events in addition to $\mathcal{G}_{u_l,t,G}^{\boldsymbol{r}_{s,u_l}^{s,t}, e_l^0}$, which is given by (4):

$$\mathcal{G}_{u_l,t,G}^{\boldsymbol{r}_{s,u_l}^{s,t}, e_l^1} = \Big\{\boldsymbol{x} \in \{0,1\}^E \mid \boldsymbol{r}_{s,u_l}^{s,t} \in \boldsymbol{r}_{s,t}, \prod_{j=1}^{|\boldsymbol{r}_{s,u_l}^{s,t}|} x_{e_j} = 1, \\ x_{e_l} = 1, \exists \boldsymbol{r}_{u_l,t} \in \mathcal{R}_{u_l,t}, \prod_{e \in \boldsymbol{r}_{u_l,t}} x_e = 1\Big\},$$

$$\mathcal{G}_{u_l,t,G}^{\boldsymbol{r}_{s,u_l}^{s,t}} = \Big\{\boldsymbol{x} \in \{0,1\}^E \mid \boldsymbol{r}_{s,u_l}^{s,t} \in \boldsymbol{r}_{s,t}, \prod_{j=1}^{|\boldsymbol{r}_{s,u_l}^{s,t}|} x_{e_j} = 1, \\ \exists \boldsymbol{r}_{u_l,t} \in \mathcal{R}_{u_l,t}, \prod_{e \in \boldsymbol{r}_{u_l,t}} x_e = 1\Big\}.$$

From the definition, $\mathcal{G}_{u_l,t,G}^{\boldsymbol{r}_{s,u_l}^{s,t}} = \mathcal{G}_{u_l,t,G}^{\boldsymbol{r}_{s,u_l}^{s,t}, e_l^0} \cup \mathcal{G}_{u_l,t,G}^{\boldsymbol{r}_{s,u_l}^{s,t}, e_l^1}$ and $\mathcal{G}_{u_l,t,G}^{\boldsymbol{r}_{s,u_l}^{s,t}, e_l^0} \cap \mathcal{G}_{u_l,t,G}^{\boldsymbol{r}_{s,u_l}^{s,t}, e_l^1} = \emptyset$. Noting that $f_{\mathrm{N}}\big(\mathcal{G}_{t,t,G}^{\boldsymbol{r}_{s,t}}, \boldsymbol{p}\big) = 1$, we can rewrite the path reliability $f_{\mathrm{P}}(\boldsymbol{r}_{s,t})$ as

$$f_{\mathrm{P}}(\boldsymbol{r}_{s,t}) = f_{\mathrm{P}}(\boldsymbol{r}_{s,t}) \cdot f_{\mathrm{N}}\big(\mathcal{G}_{t,t,G}^{\boldsymbol{r}_{s,t}}, \boldsymbol{p}\big). \tag{11}$$

If the partial path $\boldsymbol{r}_{s,u_l}^{s,t}$ of $\boldsymbol{r}_{s,t}$ is reachable and the next link e_l is unavailable, the conditional network reliability under the events $\mathcal{G}_{u_l,t,G}^{\boldsymbol{r}_{s,u_l}^{s,t}, e_l^0}$ is equivalent to that under the events $\mathcal{G}_{s,t,G}^{\boldsymbol{r}_{s,u_l}^{s,t}, e_l^0}$, and thus we have

$$f_{\mathrm{N}}\big(\mathcal{G}_{u_l,t,G}^{\boldsymbol{r}_{s,u_l}^{s,t}, e_l^0}, \boldsymbol{p}\big) = f_{\mathrm{N}}\big(\mathcal{G}_{s,t,G}^{\boldsymbol{r}_{s,u_l}^{s,t}, e_l^0}, \boldsymbol{p}\big).$$

Similarly, (11) can be rewritten as:

$$f_{\mathrm{N}}\big(\mathcal{G}_{t,t,G}^{\boldsymbol{r}_{s,t}}, \boldsymbol{p}\big) = f_{\mathrm{N}}\big(\mathcal{G}_{s,t,G}^{\boldsymbol{r}_{s,t}}, \boldsymbol{p}\big). \tag{12}$$

From (10)–(12), we have

$$f_{\mathrm{R}}(\boldsymbol{r}_{s,t}, \infty) = f_{\mathrm{P}}(\boldsymbol{r}_{s,t}) \cdot f_{\mathrm{N}}\big(\mathcal{G}_{s,t,G}^{\boldsymbol{r}_{s,t}}, \boldsymbol{p}\big) \\ + \sum_{l=1}^{H} f_{\mathrm{P}}(\boldsymbol{r}_{s,u_l}^{s,t}) \cdot (1 - p_{e_l}) \cdot \\ f_{\mathrm{N}}\big(\mathcal{G}_{s,t,G}^{\boldsymbol{r}_{s,u_l}^{s,t}, e_l^0}, \boldsymbol{p}\big). \tag{13}$$

Focusing on the last Hth link e_H, we can rewrite (13) as:

$$f_{\mathrm{R}}(\boldsymbol{r}_{s,t}, \infty) = f_{\mathrm{P}}(\boldsymbol{r}_{s,u_H}^{s,t}) \cdot p_{e_H} \cdot f_{\mathrm{N}}\big(\mathcal{G}_{s,t,G}^{\boldsymbol{r}_{s,u_H}^{s,t}, e_H^1}, \boldsymbol{p}\big) \\ + f_{\mathrm{P}}(\boldsymbol{r}_{s,u_H}^{s,t}) \cdot (1 - p_{e_H}) \cdot f_{\mathrm{N}}\big(\mathcal{G}_{s,t,G}^{\boldsymbol{r}_{s,u_H}^{s,t}, e_H^0}, \boldsymbol{p}\big) \\ + \sum_{l=1}^{H-1} f_{\mathrm{P}}(\boldsymbol{r}_{s,u_l}^{s,t}) \cdot (1 - p_{e_l}) \cdot f_{\mathrm{N}}\big(\mathcal{G}_{s,t,G}^{\boldsymbol{r}_{s,u_l}^{s,t}, e_l^0}, \boldsymbol{p}\big) \\ = f_{\mathrm{P}}(\boldsymbol{r}_{s,u_H}^{s,t}) \cdot f_{\mathrm{N}}\big(\mathcal{G}_{s,t,G}^{\boldsymbol{r}_{s,u_H}^{s,t}}, \boldsymbol{p}\big) \\ + \sum_{l=1}^{H-1} f_{\mathrm{P}}(\boldsymbol{r}_{s,u_l}^{s,t}) \cdot (1 - p_{e_l}) \cdot f_{\mathrm{N}}\big(\mathcal{G}_{s,t,G}^{\boldsymbol{r}_{s,u_l}^{s,t}, e_l^0}, \boldsymbol{p}\big).$$

By repeating the same procedure for link $e_{l'}$ in the order of $l' = H-1, \ldots, 1$, we finally obtain that the path reachability including distance-constrained detours with $\eta = \infty$ is equivalent to the s–t network reliability:

$$f_{\mathrm{R}}(\boldsymbol{r}_{s,t}, \boldsymbol{p}, \infty) = f_{\mathrm{N}}(\mathcal{G}_{s,t,G}, \boldsymbol{p}).$$

Proof to Theorem 2

Proof. As in Appendix , for simplicity of explanation, we define H as the total number of links in the path $\boldsymbol{r}_{s,t}$, i.e., $H = |\boldsymbol{r}_{s,t}|$. Please remember that the s–t diameter constrained network reliability $f_{\mathrm{N}}(\mathcal{G}_{s,t,G}(d_{s,t}^{\min} + \eta), \boldsymbol{p})$ is given by (2) and it can be rewritten as follows:.

$$
\begin{aligned}
& f_{\mathrm{N}}(\mathcal{G}_{s,t,G}(d_{s,t}^{\min}+\eta),\boldsymbol{p}) \\
&= f_{\mathrm{p}}(\boldsymbol{r}_{s,s}^{s,t})\cdot(1-p_{e_1})\cdot f_{\mathrm{N}}\big(\mathcal{G}_{s,t,G}^{\boldsymbol{r}_{s,s}^{s,t},e_0^1}(d_{s,t}^{\min}+\eta),\boldsymbol{p}\big) \\
&\quad + f_{\mathrm{p}}(\boldsymbol{r}_{s,s}^{s,t})\cdot p_{e_1}\cdot f_{\mathrm{N}}\big(\mathcal{G}_{s,t,G}^{\boldsymbol{r}_{s,s}^{s,t},e_1^1}(d_{s,t}^{\min}+\eta),\boldsymbol{p}\big) \\
&= f_{\mathrm{p}}(\boldsymbol{r}_{s,s}^{s,t})\cdot(1-p_{e_1})\cdot f_{\mathrm{N}}\big(\mathcal{G}_{s,t,G}^{\boldsymbol{r}_{s,s}^{s,t},e_0^1}(d_{s,t}^{\min}+\eta),\boldsymbol{p}\big) \\
&\quad + f_{\mathrm{p}}(\boldsymbol{r}_{s,u_2}^{s,t})\cdot(1-p_{e_2})\cdot f_{\mathrm{N}}\big(\mathcal{G}_{s,t,G}^{\boldsymbol{r}_{s,u_2}^{s,t},e_2^0}(d_{s,t}^{\min}+\eta),\boldsymbol{p}\big) \\
&\quad + f_{\mathrm{p}}(\boldsymbol{r}_{s,u_2}^{s,t})\cdot p_{e_2}\cdot f_{\mathrm{N}}\big(\mathcal{G}_{s,t,G}^{\boldsymbol{r}_{s,u_2}^{s,t},e_2^1}(d_{s,t}^{\min}+\eta),\boldsymbol{p}\big) \\
&\vdots \\
&= f_{\mathrm{p}}(\boldsymbol{r}_{s,s}^{s,t})\cdot(1-p_{e_1})\cdot f_{\mathrm{N}}\big(\mathcal{G}_{s,t,G}^{\boldsymbol{r}_{s,s}^{s,t},e_0^1}(d_{s,t}^{\min}+\eta),\boldsymbol{p}\big) \\
&\quad + f_{\mathrm{p}}(\boldsymbol{r}_{s,u_2}^{s,t})\cdot(1-p_{e_2})\cdot f_{\mathrm{N}}\big(\mathcal{G}_{s,t,G}^{\boldsymbol{r}_{s,u_2}^{s,t},e_2^0}(d_{s,t}^{\min}+\eta),\boldsymbol{p}\big) \\
&\quad \vdots \\
&\quad + f_{\mathrm{p}}(\boldsymbol{r}_{s,u_H}^{s,t})\cdot(1-p_{e_H})\cdot f_{\mathrm{N}}\big(\mathcal{G}_{s,t,G}^{\boldsymbol{r}_{s,u_H}^{s,t},e_H^0}(d_{s,t}^{\min}+\eta),\boldsymbol{p}\big) \\
&\quad + f_{\mathrm{p}}(\boldsymbol{r}_{s,u_H}^{s,t})\cdot p_{e_H}\cdot f_{\mathrm{N}}\big(\mathcal{G}_{s,t,G}^{\boldsymbol{r}_{s,u_H}^{s,t},e_H^1}(d_{s,t}^{\min}+\eta),\boldsymbol{p}\big) \\
&= \sum_{l=1}^{H} f_{\mathrm{p}}(\boldsymbol{r}_{s,u_l}^{s,t})\cdot(1-p_{e_l})\cdot f_{\mathrm{N}}\big(\mathcal{G}_{s,t,G}^{\boldsymbol{r}_{s,u_l}^{s,t},e_l^0}(d_{s,t}^{\min}+\eta),\boldsymbol{p}\big) \\
&\quad + f_{\mathrm{p}}(\boldsymbol{r}_{s,t})\cdot f_{\mathrm{N}}\big(\mathcal{G}_{s,t,G}^{\boldsymbol{r}_{s,t}}(d_{s,t}^{\min}+\eta),\boldsymbol{p}\big) \\
&= f_{\mathrm{p}}(\boldsymbol{r}_{s,t}) \\
&\quad + \sum_{l=1}^{H} f_{\mathrm{p}}(\boldsymbol{r}_{s,u_l}^{s,t})\cdot(1-p_{e_l})\cdot f_{\mathrm{N}}\big(\mathcal{G}_{s,t,G}^{\boldsymbol{r}_{s,u_l}^{s,t},e_l^0}(d_{s,t}^{\min}+\eta),\boldsymbol{p}\big).
\end{aligned}
\tag{14}
$$

On the other hand, the path reachability including the distance-constrained detours of $\boldsymbol{r}_{s,t}$, $f_{\mathrm{R}}(\boldsymbol{r}_{s,t},\boldsymbol{p},d_{s,t}^{\min}+\eta)$ is given by (9). By comparing (9) with (14), we observe that only the last term is different between them and the following condition always holds for every $l=1,\dots,H$:

$$
\begin{aligned}
f_{\mathrm{N}}\big(\mathcal{G}_{u_l,t,G}^{\boldsymbol{r}_{s,u_l}^{s,t},e_l^0}(d_{s,t}^{\min}+\eta-f_{\mathrm{d}}(\boldsymbol{r}_{s,u_l}^{s,t})),\boldsymbol{p}\big) \le \\
f_{\mathrm{N}}\big(\mathcal{G}_{s,t,G}^{\boldsymbol{r}_{s,u_l}^{s,t},e_l^0}(d_{s,t}^{\min}+\eta),\boldsymbol{p}\big).
\end{aligned}
$$

References

1. Boesch FT, Satyanarayana A and Suffel CL. A Survey of Some Network Reliability Analysis and Synthesis Results. *Networks: An International Journal* 2009; 54(2): 99–107.
2. Gertsbakh IB and Shpungin Y. *Models of Network Reliability: Analysis, Combinatorics, and Monte Carlo*. Florida: CRC press, 2016.
3. Inoue T. Reliability Analysis for Disjoint Paths. *IEEE Transactions on Reliability* 2018; 68(3): 985–998.
4. Hara T, Sasabe M and Kasahara S. Geographical Risk Analysis Based Path Selection for Automatic, Speedy, and Reliable Evacuation Guiding Using Evacuees' Mobile Devices. *Journal of Ambient Intelligence and Humanized Computing* 2019; 10(6): 2291–2300.
5. Petingi L and Rodriguez J. Reliability of Networks with Delay Constraints. *Congressus Numerantium* 2001; 152: 117–124.
6. Kasai Y, Sasabe M and Kasahara S. Congestion-Aware Route Selection in Automatic Evacuation Guiding Based on Cooperation between Evacuees and Their Mobile Nodes. *EURASIP Journal on Wireless Communications and Networking* 2017; 2017(164): 1–11.
7. Komatsu N, Sasabe M, Kawahara J et al. Automatic Evacuation Guiding Scheme Based on Implicit Interactions between Evacuees and Their Mobile Nodes. *GeoInformatica* 2018; 22(1): 127–141.
8. Hardy G, Lucet C and Limnios N. K-Terminal Network Reliability Measures with Binary Decision Diagrams. *IEEE Transactions on Reliability* 2007; 56(3): 506–515.
9. Xiang S and Yang J. k-Terminal Reliability of Ad Hoc Networks Considering the Impacts of Node Failures and Interference. *IEEE Transactions on Reliability* 2020; 69(2): 725–739.
10. Ball MO. Computational Complexity of Network Reliability Analysis: An Overview. *IEEE Transactions on Reliability* 1986; 35(3): 230–239.
11. Canale E, Cancela H, Robledo F et al. Diameter Constrained Reliability: Complexity, Distinguished Topologies and Asymptotic Behavior. *Networks* 2015; 66(4): 296–305.
12. Rosenthal A. Computing the Reliability of Complex Networks. *SIAM Journal on Applied Mathematics* 1977; 32(2): 384–393.
13. Abraham J. An Improved Algorithm for Network Reliability. *IEEE Transactions on Reliability* 1979; R-28(1): 58–61.
14. Mo Y, Liang M, Xing L et al. Network Simplification and K-Terminal Reliability Evaluation of Sensor-Cloud Systems. *IEEE Access* 2020; 8: 177206–177218.
15. Reed S, Löfstrand M and Andrews J. An Efficient Algorithm for Computing Exact System and Survival Signatures of K-Terminal Network Reliability. *Reliability Engineering & System Safety* 2019; 185: 429–439.
16. Fishman GS. A Monte Carlo Sampling Plan for Estimating Network Reliability. *Operations Research* 1986; 34(4): 581–594.
17. L'Ecuyer P, Rubino G, Saggadi S et al. Approximate Zero-Variance Importance Sampling for Static Network Reliability Estimation. *IEEE Transactions on Reliability* 2011; 60(3): 590–604.
18. Paredes R, Dueñas-Osorio L, Meel KS et al. Principled Network Reliability Approximation: A Counting-Based Approach. *Reliability Engineering & System Safety* 2019; 191: 106472.
19. Li D, Zhang Q, Zio E et al. Network Reliability Analysis Based on Percolation Theory. *Reliability Engineering & System Safety* 2015; 142: 556–562.
20. Bunde A and Havlin S. *Fractals and Disordered Systems*. Springer Science & Business Media, 2012.
21. Stauffer D and Aharony A. *Introduction to Percolation Theory*. CRC press, 2018.
22. Kuo SY, Yeh FM and Lin HY. Efficient and Exact Reliability Evaluation for Networks with Imperfect Vertices. *IEEE Transactions on Reliability* 2007; 56(2): 288–300.
23. Walteros JL and Pardalos PM. Selected Topics in Critical Element Detection. In *Applications of Mathematics and Informatics in Military Science*. Berlin Heidelberg: Springer, 2012. pp. 9–26.
24. Ahuja R. *Network Flows: Theory, Algorithms, and Applications*. Englewood Cliffs, N.J: Prentice Hall, 1993.
25. Yick J, Mukherjee B and Ghosal D. Wireless Sensor Network Survey. *Computer Networks* 2008; 52(12): 2292–2330.

26. Zonouz AE, Xing L, Vokkarane VM et al. Reliability-Oriented Single-Path Routing Protocols in Wireless Sensor Networks. *IEEE Sensors Journal* 2014; 14(11): 4059–4068.
27. Nowsheen N, Karmakar G and Kamruzzaman J. PRADD: A Path Reliability-Aware Data Delivery Protocol for Underwater Acoustic Sensor Networks. *Journal of Network and Computer Applications* 2016; 75: 385–397.
28. Chatterjee S and Das S. Ant Colony Optimization Based Enhanced Dynamic Source Routing Algorithm for Mobile Ad-Hoc Network. *Information Sciences* 2015; 295: 67–90.
29. Kumar BVS and Padmavathy N. A Hybrid Link Reliability Model for Estimating Path Reliability of Mobile Ad Hoc Network. *Procedia Computer Science* 2020; 171: 2177–2185.
30. Huang H, Yin H, Min G et al. Energy-Aware Dual-Path Geographic Routing to Bypass Routing Holes in Wireless Sensor Networks. *IEEE Transactions on Mobile Computing* 2017; 17(6): 1339–1352.
31. Lima MM, Oliveira HA, Guidoni DL et al. Geographic Routing and Hole Bypass Using Long Range Sinks for Wireless Sensor Networks. *Ad Hoc Networks* 2017; 67: 1–10.
32. Beccuti M, Bobbio A, Franceschinis G et al. A New Symbolic Approach for Network Reliability Analysis. In *Proc. of IEEE/IFIP International Conference on Dependable Systems and Networks (DSN 2012)*. pp. 1–12.
33. Bryant RE. Graph-Based Algorithms for Boolean Function Manipulation. *IEEE Transactions on Computers* 1986; 100(8): 677–691.
34. Inoue T, Iwashita H, Kawahara J et al. Graphillion: Software Library for Very Large Sets of Labeled Graphs. *International Journal on Software Tools for Technology Transfer* 2016; 18(1): 57–66.
35. Minato S. Zero-Suppressed BDDs and Their Applications. *International Journal on Software Tools for Technology Transfer* 2001; 3(2): 156–170.
36. Clark BN, Colbourn CJ and Johnson DS. Unit Disk Graphs. In *Annals of Discrete Mathematics*, volume 48. Amsterdam: Elsevier, 1991. pp. 165–177.
37. Hoffmann S and Wanke E. Generic Route Repair: Augmenting Wireless Ad Hoc Sensor Networks for Local Connectivity. In *Proc. of 2016 15th ACM/IEEE International Conference on Information Processing in Sensor Networks (IPSN)*. pp. 1–10.
38. Khallef W, Molnar M, Benslimane A et al. Multiple Constrained QoS Routing with RPL. In *Proc. of 2017 IEEE International Conference on Communications (ICC)*. pp. 1–6.
39. Malboubi M, Vu C, Chuah CN et al. Compressive Sensing Network Inference with Multiple-Description Fusion Estimation. In *Proc. of 2013 IEEE Global Communications Conference (GLOBECOM)*. pp. 1557–1563.
40. City of Nagoya. Earthquake-Resistance City Development Policy (in Japanese). http://www.city.nagoya.jp/jutakutoshi/cmsfiles/contents/0000002/2717/honpen.pdf, 2015. Accessed 14 Jan. 2021.
41. Hara T, Sasabe M, Matsuda T et al. Capacitated Refuge Assignment for Speedy and Reliable Evacuation. *ISPRS International Journal of Geo-Information* 2020; 9(7): 442: 1–19.

Supplemental material

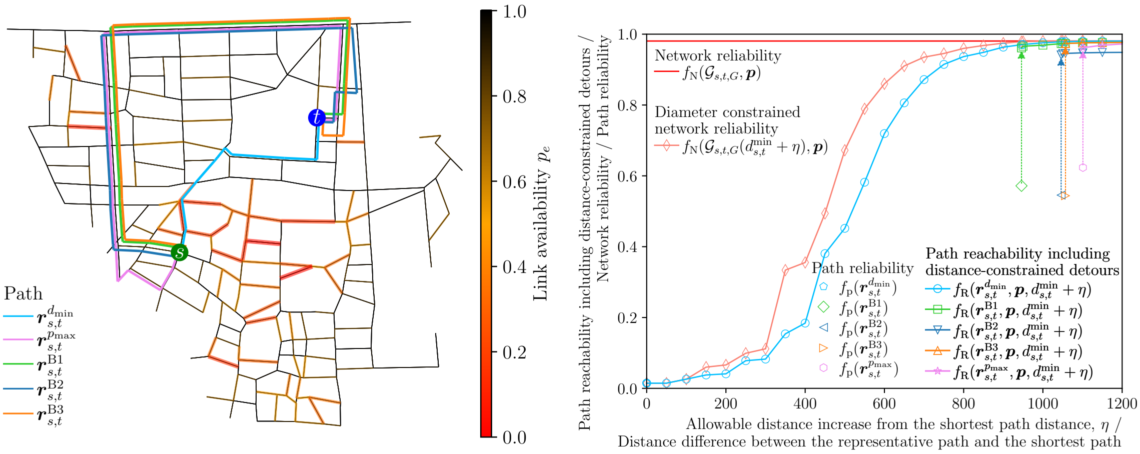

(a) Network topology and five representative paths.

(b) Impact of η on path reachability including distance-constrained detours.

Figure 10. Results of road network (Area 1, $s = s_{1,2}, t = t_1$).

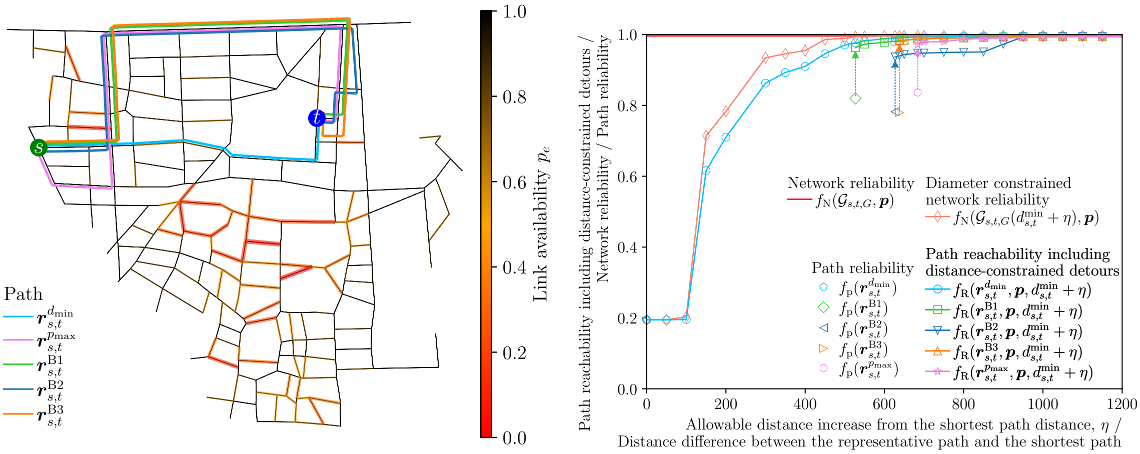

(a) Network topology and five representative paths.

(b) Impact of η on path reachability including distance-constrained detours.

Figure 11. Results of road network (Area 1, $s = s_{1,3}, t = t_1$).

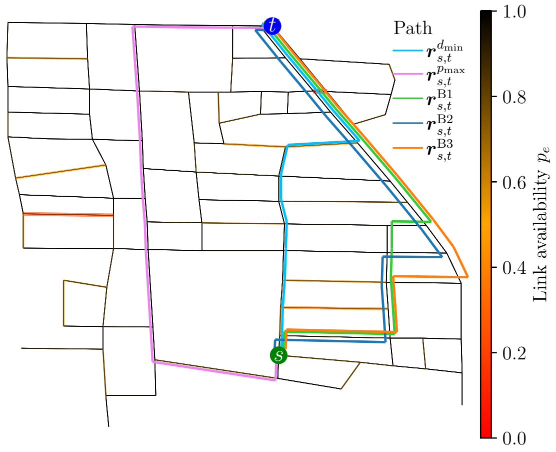

(a) Network topology and five representative paths.

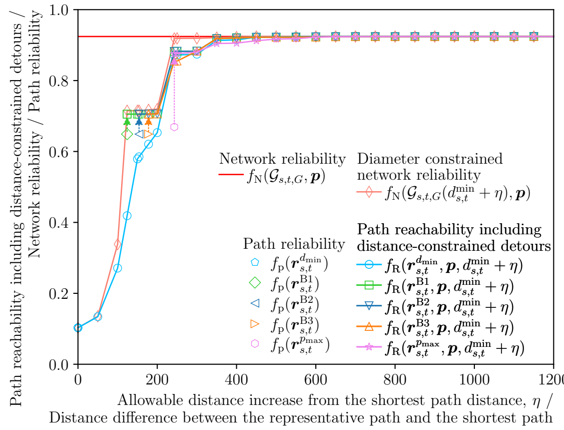

(b) Impact of η on path reachability including distance-constrained detours.

Figure 12. Results of road network (Area 2, $s = s_{2,1}, t = t_2$).

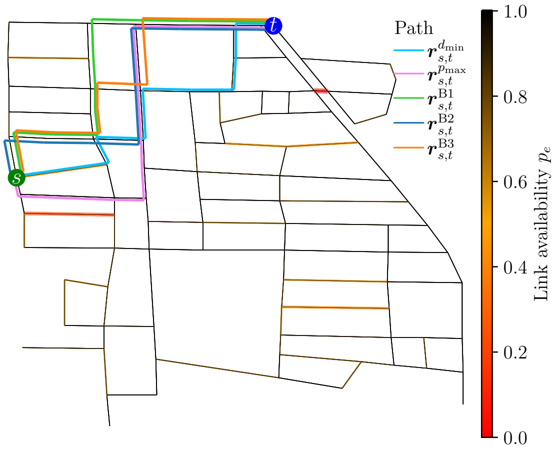

(a) Network topology and five representative paths.

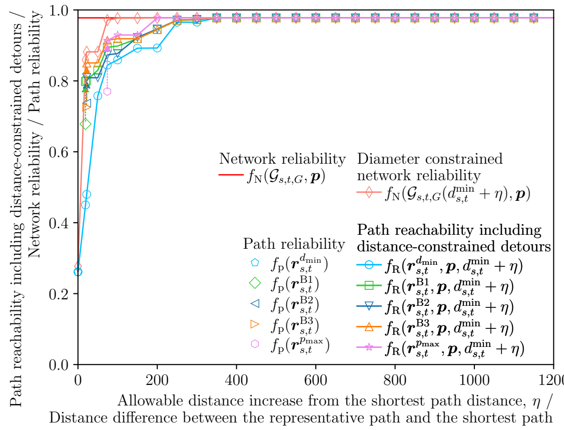

(b) Impact of η on path reachability including distance-constrained detours.

Figure 13. Results of road network (Area 2, $s = s_{2,2}, t = t_2$).

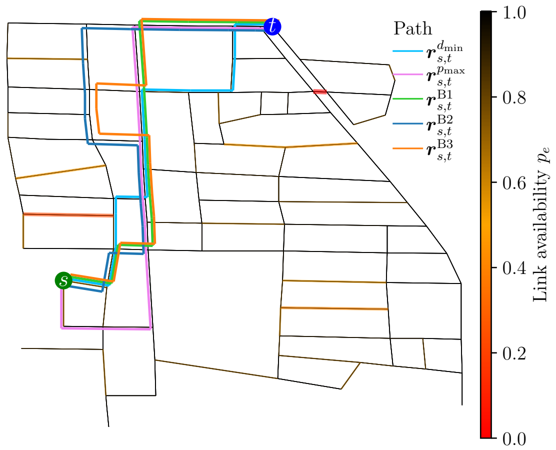

(a) Network topology and five representative paths.

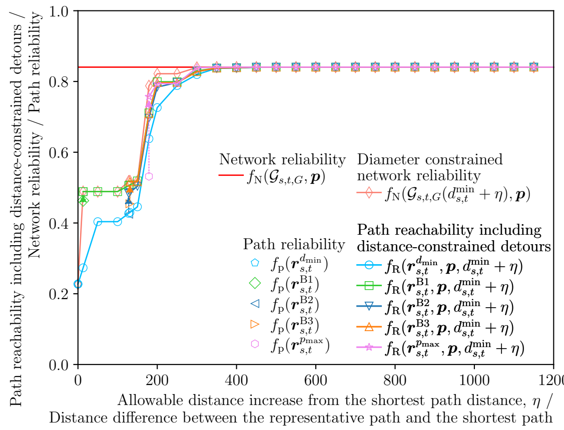

(b) Impact of η on path reachability including distance-constrained detours.

Figure 14. Results of road network (Area 2, $s = s_{2,3}, t = t_2$).

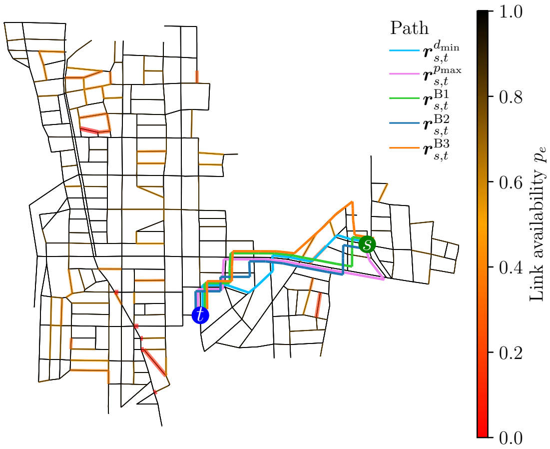

(a) Network topology and five representative paths.

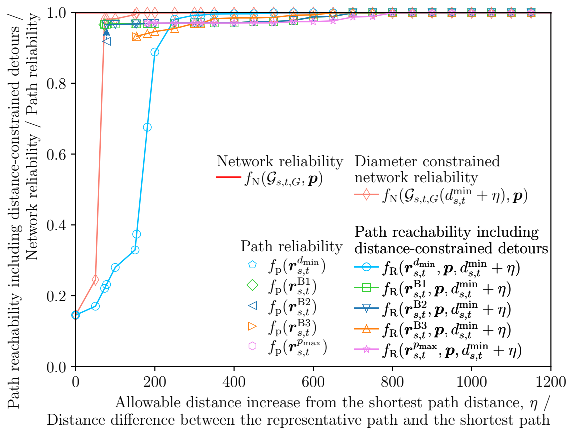

(b) Impact of η on path reachability including distance-constrained detours.

Figure 15. Results of road network (Area 3, $s = s_{3,1}, t = t_3$).

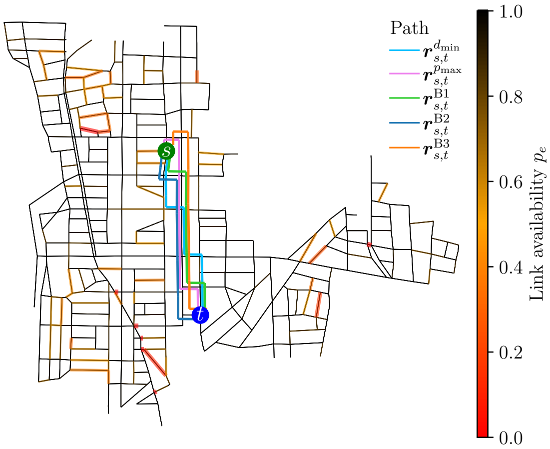

(a) Network topology and five representative paths.

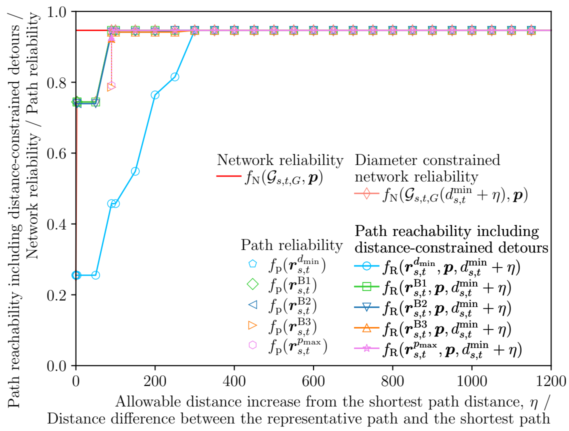

(b) Impact of η on path reachability including distance-constrained detours.

Figure 16. Results of road network (Area 3, $s = s_{3,2}, t = t_3$).

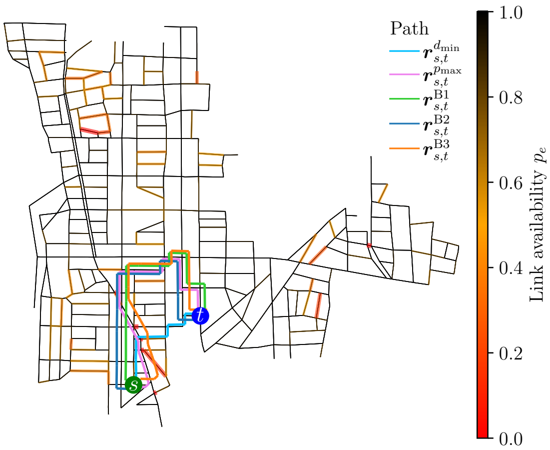

(a) Network topology and five representative paths.

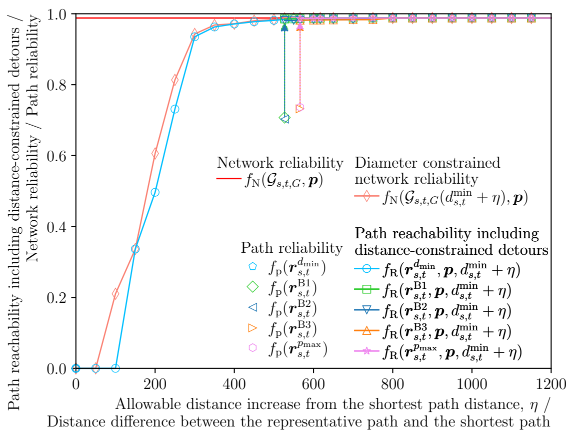

(b) Impact of η on path reachability including distance-constrained detours.

Figure 17. Results of road network (Area 3, $s = s_{3,3}, t = t_3$).